Active bath-induced localization and collapse of passive semiflexible polymers

S. Mahdiyeh Mousavi, Gerhard Gompper, and Roland G. Winkler*
Theoretical Physics of Living Matter, Institute for Advanced Simulation and Institute of Biological Information Processing, Forschungszentrum Jülich, D-52425 Jülich, Germany

The conformational and dynamical properties of a passive polymer embedded in a bath of active Brownian particles (ABPs) are studied by Langevin dynamics simulations. Various activities and ABP concentrations below and above the critical values for motility-induced phase separation (MIPS) are considered. In a homogeneous ABP fluid, the embedded polymer swells with increasing bath activity, with stronger swelling for larger densities. The polymer dynamics is enhanced, with the diffusion coefficient increasing by a power-law with increasing activity, where the exponent depends on the ABP concentration. For ABP concentrations in the MIPS regime, we observe a localization of the polymer in the low-density ABP phase associated with polymer collapse for moderate activities, and a reswelling for high activities accompanied by a preferred localization in the high density ABP phase. Localization and reswelling is independent of the polymer stiffness, with stiff polymers behaving similarly to flexible polymers. The polymer collapse is associated with a slowdown of its dynamics and a significantly smaller center-of-mass diffusion coefficient. In general, the polymer dynamics can only partially be described by an effective (bath) temperature. Moreover, the properties of a polymer embedded in an homogeneous active bath deviate quantitatively from those of a polymer composed of active monomers, i.e., linear chains of ABPs; however, such a polymer exhibits qualitatively similar activity-dependent features.

I. INTRODUCTION

Active matter exhibits remarkable cooperative and collective phenomena, such as swarming and active turbulence of bacteria [1–13], and activity-induced phase separation of synthetic Janus-swimmers [13–22], which are absent in passive counterparts. In large-scale simulations of active Brownian particles (ABPs) [15, 16, 23] — self-propelled (hard-sphere-type) spherical colloids — motility-induce phase separation (MIPS) has been found and phase diagrams been determined for systems in two [21, 22, 24] and three dimensions [20, 21, 24, 25]. Here, activity yields a separation of the active fluid into a dense and dilute phase.

Mixtures of active and passive particles (PP) show even more intriguing effects. Hydrodynamic and steric interactions yield an enhanced diffusive motion of passive (colloidal) tracer particles immersed in a bath of active agents [26–39]. Simulations of two-dimensional (2D) binary mixtures of isometric passive and active particles yield for sufficiently strong activities and active particle densities phase separation and formation of dense passive clusters, which are encased by layers of active particles [40–44]. Similarly, large athermal passive colloids in a mixtures with small active particles reveal an effective depletion-like attraction by the interactions with the small particles and a phase separation [45]. Phase separation can also be achieved by a fixed temperature difference [46] between two species of particles [47]. Yet, in contrast to mixtures of ABPs/passive colloids, no encasing active-particle layer seems to appear in this case, which indicates a qualitatively different driving mechanism for the phase separation. Simulations provide evidence of an emergent collective dynamics in phase-separated mixtures of isometric active and passive Brownian particles, with a novel steady-state of propagating interfaces [42]. This emphasizes the tight dynamical coupling between the two types of particles, which certainly depends on the mechanism maintaining their out-of-equilibrium character.

The presence of both active and passive components is a hallmark of living systems [48–52]. The motility of microorganisms plays an essential role in maintaining an ecological balance and achieving biomixing of nutrients in aqueous environments [33, 53, 54]. The enhanced diffusion of a variety of passive particles, such as enzymes, granules, or extracellular products, either by ATP consumption and cyclic conformational changes as for proteins, their coupling to other biomolecules, e.g., DNA and RNA, or by induced hydrodynamic flows, is essential for the proper function of a cell and promotes intercellular signaling and metabolite transports [55–60]. So far, the impact of activity on the properties of the passive components has not yet received the attention it deserves. Simulations of two-component mixtures of polymers at different temperatures yield phase separation [61]. Here, the two temperatures account for example for the activity of hetero- and euchromatin, which could play a role in chromation separation in the cell nucleus [61–65]. There are a variety of other out-of-equilibrium processes in a cell, which merit awareness. Cells exhibit coherent structures — so-called membraneless organelles or condensates — encompassing and concentrating specific molecules such as proteins and RNA in the cytoplasm [66–68]. *In-vivo* experiments suggest that active processes, which occur constantly within such organelles, play a role in their formation [66, 67]. Insight into the interplay between equilibrium thermodynamic driving forces and nonequi-

* g.gompper@fz-juelich.de, r.winkler@fz-juelich.de

librium activity in the process of organelle formation is fundamental to reveal their functional properties, and to elucidate their contribution to cell physiology and diseases.

Anisotropic shapes and internal degrees of freedom of passive particles in an active bath yield further effects absent in pure passive systems. Ellipsoids embedded in an *E. coli* suspension show an anomalous coupling between the ellipsoid's translational and rotational motion, which is strictly prohibited in thermal equilibrium [37]. Passive semiflexible polymers embedded in an active bath of ABPs exhibit novel transient states in 2D [69–73], where an activity-induced bending of the polymers implies an asymmetric exposure to active particles, with ABPs accumulating in regions of highest curvature, as has been observed for ABPs in confinement [19]. This leads to particular polymer conformations such as hairpins, structures which are only temporarily stable and dissolve and rebuild in the course of time.

In this article, we consider the properties of semiflexible polymers embedded in an three-dimensional (3D) ABP fluid. Compared to 2D systems, the additional spatial dimension removes constraints on the ABPs' degrees of freedom and 2D-characteristic transient states are no longer present. We analyze the conformational and transport properties of the passive polymers as a function of the bath density and activity. Specifically, we consider a homogeneous bath (no MIPS or clusters) and compare the polymer properties with those in a phase separated fluid (MIPS). As for mixtures of active and passive colloids, in the homogeneous phase, we find an enhanced diffusive motion of the polymer — an anomalous diffusion at short times and an activity-driven diffusive motion at long times. Flexible polymers swell and semiflexible polymers shrink at smaller activities, and semiflexible polymers swell at larger activities similar to flexible polymers. An equivalent behavior is obtained for dry active polymers composed of ABP monomers (ABPO) exposed to colored noise [74–77]. However, there are significant quantitative differences between the conformational and dynamical characteristics of ABPOs and polymers embedded in the active bath. The latter show a less pronounced dependence on activity. This is not surprising, because the active ABP bath does not strictly mimic colored noise, in the sense of an exponentially decaying noise correlation function [78], the bath-induced active motion rather decays faster, and correspondingly affects polymer conformations to a less extent.

In case of the phase-separated active fluid (MIPS), most remarkably, we find an activity-dependent localization of (semiflexible) polymers in the low-fluid-density ABP region. This is accompanied with a collapse of the polymer manifested by a mean-square end-to-end distance comparable to that of a flexible polymer in a passive bath. This also affects the polymer dynamics and the center-of-mass diffusion coefficient is substantially lower than that predicted in absence of localization. Stronger active noise leads to a dissolution of the polymer in the high-density ABP phase, with a swelling of the polymer and an enhanced dynamics. Interestingly, this behavior is independent of polymer stiffness.

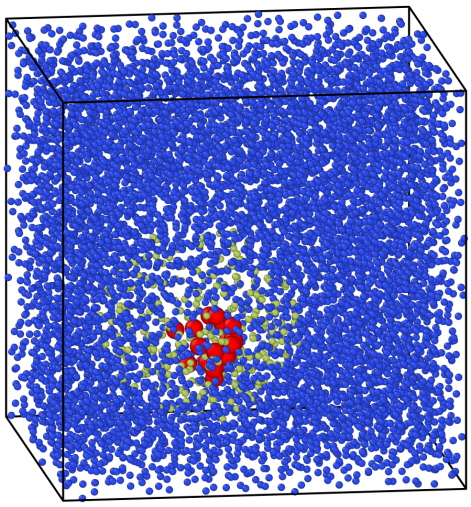

FIG. 1. Simulation snapshot of a polymer (red) immersed in bath of ABPs (blue, green) at the Péclet number $Pe = 100$. The size of the ABPs is reduced to illustrate the density inhomogeneity and for visibility of the polymer. The polymer is localized in the "bubble" of the low-density MIPS phase. The ABPs inside the spherical bubble of radius 5.5σ with the polymer center-of-mass as center are colored in green. (See movie M1 of the supplementary material for illustration.)

The article is organized as follows. Section II describes the model for the ABP active bath and the polymer. The properties of bare ABP fluids as well as fluid mixtures of passive and active particles are briefly addressed in Sec. III. Results for the conformational and dynamical properties of semiflexible polymers embedded in ABP baths of various concentrations are presented in Sec. IV. Finally, Sec. V summarizes our findings and presents our conclusions.

II. MODEL

A. Active Brownian particle

We consider a three-dimensional system of N_a ABPs in a cubic box of length L_b with periodic boundary conditions. The ABPs are modeled as colloidal particles of mass m, diameter σ, and self-propulsion velocity v_0 along the fixed direction $\boldsymbol{e}_i$, $i = 1, \ldots, N$ [15, 16, 79, 80]. The translational motion of their positions $\boldsymbol{r}_i$ is described by the Langevin equations

$$m\ddot{\boldsymbol{r}}_i(t) = \gamma\left[v_0\boldsymbol{e}_i(t) - \dot{\boldsymbol{r}}_i(t)\right] + \boldsymbol{F}_i(t) + \boldsymbol{\Gamma}_i(t), \qquad (1)$$

with the translational friction coefficient γ and the forces $\boldsymbol{F}_i$ on particle i by excluded-volume interactions between ABPs and monomers of a polymer (cf. Eq. (8)). The

change of the propulsion directions, $\boldsymbol{e_i}$, is given by

$$\dot{\boldsymbol{e}}_i(t) = \boldsymbol{\Xi}_i(t) \times \boldsymbol{e}_i(t). \tag{2}$$

The $\boldsymbol{\Gamma}_i$ and $\boldsymbol{\Xi}_i$ are Gaussian and Markovian stochastic processes with zero mean and the second moments

$$\langle \Gamma_{\alpha i}(t)\, \Gamma_{\beta j}(t')\rangle = 2\gamma k_B T \delta_{\alpha\beta}\delta_{ij}\delta(t-t'), \tag{3}$$
$$\langle \Xi_{\alpha i}(t)\, \Xi_{\beta j}(t')\rangle = 2D_R \delta_{\alpha\beta}\delta_{ij}\delta(t-t'), \tag{4}$$

with the temperature T, the Boltzmann constant k_B, the rotational diffusion coefficient D_R, and the Cartesian coordinates $\alpha, \beta \in \{x, y, z\}$. Equation (4) yields the correlation function of the propulsion direction [15, 81]

$$\langle \boldsymbol{e}_i(t) \cdot \boldsymbol{e}_j(0)\rangle = e^{-2D_R t}\delta_{ij}. \tag{5}$$

For a three-dimensional colloid in a fluid, the thermal translational, $D_T = k_B T/\gamma$, and the rotational, D_R, diffusion coefficients are related according to $D_T/\sigma^2 D_R = 1/3$ [81].

B. Passive polymer

A polymer is modeled as a bead-spring chain of N_m monomers, with monomers of the same size and mass as ABPs. Their equations of motion are given by Eq. (1) without the active force, i.e., $v_0 = 0$. The forces $\boldsymbol{F}_k = -\partial U/\partial \boldsymbol{r}_k$ $(k = 1, \ldots, N_m)$, comprise contributions from potentials by bonds, U_l, bending, U_b, and excluded-volume interactions, U_{ex}, i.e., $U = U_l + U_b + U_{ex}$, with the potentials

$$U_l = \frac{k_l}{2} \sum_{k=1}^{N_m - 1} \left(|\boldsymbol{R}_k| - l\right)^2, \tag{6}$$

where $\boldsymbol{R}_k = \boldsymbol{r}_{k+1} - \boldsymbol{r}_k$ is the bond vector connecting neighboring monomers, k_l the spring constant, and l the rest length of a bond,

$$U_b = \frac{k_b}{2} \sum_{k=1}^{N_m - 2} (\boldsymbol{R}_{k+1} - \boldsymbol{R}_k)^2, \tag{7}$$

with the bending constant k_b, and

$$U_{ex}(r) = \begin{cases} 4\epsilon \left[\left(\frac{\sigma}{r}\right)^{12} - \left(\frac{\sigma}{r}\right)^{6} + \frac{1}{4} \right], & r < r_c = \sqrt[6]{2}\sigma \\ 0, & r > r_c \end{cases}, \tag{8}$$

with r the distance between particles and ϵ the interaction strength.

The equations of motion (1) are integrated with a velocity Verlet-type scheme [82]. The procedure to solve Eq. (2) is described in Refs. [81, 83].

C. Parameters

In the simulation, we measure energies in units of the thermal energy $k_B T$, lengths in units of the equilibrium bond length $\sigma = l$, and time in units of $\tau = \sqrt{m\sigma^2/(k_B T)}$. The activity of the ABPs is characterized by the Péclet number

$$Pe = \frac{v_0}{\sigma D_R}, \tag{9}$$

and the ratio $\Delta = D_T/(\sigma^2 D_R) = 1/3$ is used. Explicitly, we choose $\gamma = 50\sqrt{m k_B T/\sigma^2}$, which yields the rotational diffusion coefficient $D_R = 0.06/\tau$. This choice of the friction coefficient ensures overdamped motion on time scales $t \gg 1/\gamma$. To prevent bond stretching and an activity-dependent overlap between ABPs and monomers, respectively, we set $k_l = (5+Pe)\times 10^3 k_B T/\sigma^2$ and $\epsilon = (Pe+1)k_B T$, which implies bond-length variations smaller than 3% of the equilibrium value l and a nearly Pe-independent nearest-neighbor distance. The density of ABPs is measured in terms of the global packing fraction $\phi = \pi\sigma^3 N/(6L_b^3)$, with L_b the length of the cubic simulation box. We study a single polymer with $N_m = 20$ monomers, hence, length $L = 19l$, in a system of size $L_b = 22\sigma$ for the ABP packing fractions $\phi \approx 0.13$, 0.27, and 0.53.

In the integration of Eq. (1) and (2), the time step $\Delta t = 5\times 10^{-4}\tau$ is applied. For every Péclet number, simulations are performed for 10^8 time steps, corresponding to the total time $T_t = 5\times 10^4 \tau$ — or $T_t D_R = 3\times 10^3$ —, and up to 8 realizations are considered.

III. PROPERTIES OF ACTIVE-PASSIVE MIXTURES

A remarkable feature of an active fluid is MIPS, which for ABPs in 3D leads to a phase separation into a dense and a dilute fluid phase above a critical density and Péclet number [20, 21, 24, 25]. Here, the Péclet number (9), needs to exceed the value $Pe \approx 30$, and the packing fraction the value $\phi \approx 0.35$ for $Pe \lesssim 300$ [20, 42]. Simulations of pure ABP fluids with the current setup confirm these results. Figure 1 illustrates the coexistence of a high-density and low-density fluid region.

The presence of passive particles (PPs) in isometric mixtures with ABPs changes the critical Péclet number as well as the critical overall packing fraction (ABPs + PPs) for MIPS [42, 43]. Simulations of 2D mixtures yield a shift of these critical quantities to larger values. However, the studies of Ref. [42] suggest that the critical packing fraction of ABPs for MIPS in mixtures is independent of the concentration of PPs and needs to exceed the critical ABP value in absence of PPs. Our current studies on 3D mixtures confirm the 2D observations.

To illustrate the effect of the active bath on the properties of PPs (monomers) in a mixture, we analyze their diffusive behavior. Figure 2 presents the mean-square

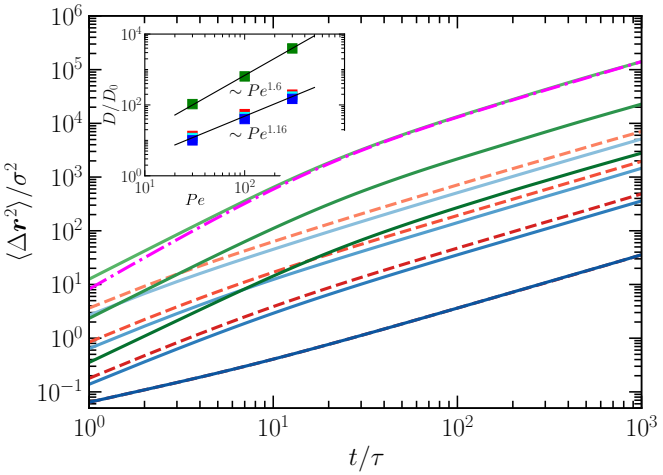

FIG. 2. Mean-square displacement of APBs (green) and PPs (blue, red) in an active bath with the average particle packing fraction $\phi = 0.53$, the PP fractions $N_p/N = 0.3$ (red, dashed) and 0.5 (blue), and the Péclet numbers $Pe = 0.01$, 30, 100, and 300 (dark to bright). The magenta dashed-dotted line indicates the MSD of an ABP with the rotational diffusion coefficient $D_R = 0.06/\tau$ and the effective Péclet number $Pe = 48.7$. The MSD for $Pe = 0.01$ is identical for all considered cases. Inset: long-time active diffusion coefficients for ABPs (green) and passive particles in the active bath for $N_p/N = 0.3$ (red), 0.4 (cyan), and 0.5 (blue) as a function of the Péclet number. The ABP diffusion coefficients are independent of the fraction N_p/N. The solid lines indicate power-laws with the exponent 1.60 (ABPs) and 1.16 (PPs), respectively. $D_0 = 0.006\sigma^2/\tau$ is the diffusion coefficient of the particles in the passive system.

displacement (MSD) $\langle \Delta \boldsymbol{r}_i^2(t) \rangle = \langle (\boldsymbol{r}_i(t) - \boldsymbol{r}_i(0))^2 \rangle$ of PPs and ABPs in mixtures for various fractions N_p/N of PPs, where N_p is the number of PPs and $N = N_p + N_a$ is the total number of particles, and various Péclet numbers at the overall packing fraction $\phi = 0.53$. Note that a pure ABP fluid is phase separated for this packing fraction. Yet, the ABP concentrations $N_p/N = 0.3$, 0.4, and 0.7, in our considered mixtures, are too small to exhibit MIPS. Evidently, the passive-particle dynamics is activity enhanced, with MSDs increasing with increasing bath activity, Pe. However, the enhancement is significantly smaller than that of ABPs. As for the latter, we obtain a short time super-diffusive behavior, which turns into an active diffusion for long times. However, the exponent in the super-diffusive regime is significantly smaller than 2, the value of ABPs in dilute systems [15].

The magenta line in Fig. 2 indicates a fit of the MSD of the ABPs at $Pe = 300$ by the expression [15]

$$\left\langle \Delta \boldsymbol{r}^2(t) \right\rangle = \frac{\sigma^2 Pe^2}{2} \left(2D_R t + \exp(-2D_R t) - 1\right) \qquad (10)$$

of an ABP in a dilute system. This expression yields a crossover from an active ballistic short-time motion to a long-time diffusive MSD at $2D_R t \approx 1$ with the diffusion coefficient $D = \sigma^2 D_R Pe^2/6$ [15]. Since the rotational diffusion is an independent stochastic process, the ABPs in the mixtures follow the predicted crossover. However, the ABP dynamics is significantly slowed down. As indicated by the fit, the extracted effective Péclet number $Pe = 48.7$ is significantly smaller than that of an ABP in dilute solution, $Pe = 300$, since the interactions between ABPs and PPs reduce the ABP swim velocity. Moreover, the inset of Fig. 2 reveals a power-law increase of the active diffusion coefficient, D, with the exponent 1.6, smaller that the theoretical value 2. In addition, the short-time dynamics is super-diffusive, but not ballistic. These facts reflect the influence of the finite overall particle density on the ABP dynamics. Noteworthy, the ABP properties are independent of the actual composition of the mixture at the constant packing fraction ϕ.

The activity dependence of the passive-particle diffusion coefficient $D \sim Pe^{1.16}$ is even weaker than that of the ABPs (Fig. 2). Moreover, an increasing fraction of passive particles reduces the value of D for the considered range of Pe; the diffusion coefficients at $N_p/N = 0.3$ are approximately 30% larger than those at $N_p/N = 0.5$, independent of Pe.

In contrast to the ABPs, the PPs show no persistent motion. The calculation of the PP velocity correlation function yields a nearly instantaneous decay of the correlation function, roughly as for particles exposed to white noise. Nevertheless, PPs show a crossover from a short-time super-diffusive behavior to long-time diffusion, which is clearly governed by interactions with ABPs. The activity-enhanced dynamics at larger Pe leads to a shift of the crossover to shorter times by approximately a factor of two between $Pe = 300$ and 30 for any fraction of passive particles. This reflects that the PP dynamics induced by the bath is significantly different from that of self-propelled particles, despite qualitatively similar features.

IV. PASSIVE POLYMER IN ACTIVE BATH

A. Polymer conformational properties

The polymer properties strongly depend on the ABP concentration. Particular effects appear for concentrations above the critical value for MIPS, $\phi \approx 0.34$, and $Pe \lesssim 300$ (cf. Fig. 3). Since we focus on a single short polymer with $N_m = 20$, the monomer concentration plays a negligible role for the overall concentration of particles in the system.

1. *Low ABP concentration regime — homogeneous fluid*

In the low-concentration regime, we consider the ABP packing fractions $\phi = 0.13$ and $\phi = 0.27$, the ABP fluid is homogeneous and isotropic (cf. Fig. 3). As illustrated in Fig. 4 for the polymer mean-square end-to-end distance $\langle \boldsymbol{R}_e^2 \rangle = \langle (\boldsymbol{r}_N - \boldsymbol{r}_1)^2 \rangle$, the active bath generates a

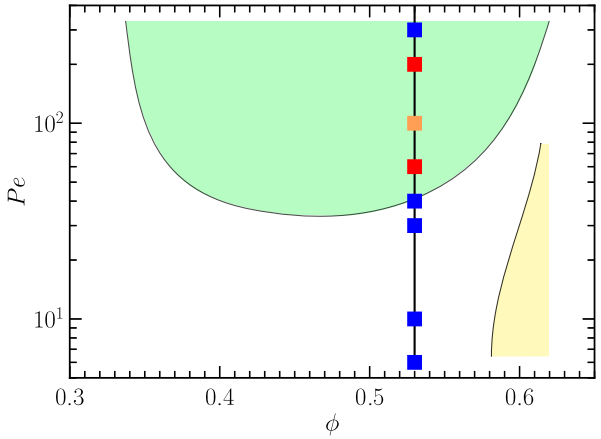

FIG. 3. Illustration of the phase diagram of active Brownian particles in three dimensions as a function of the Péclet number and the packing fraction. The shaded areas indicate the liquid–gas (light green) and the crystal–gas (light yellow) coexistence regimes [20, 81]. Symbols represent the considered Péclet numbers for the simulations of a passive polymer in the active bath. Blue squares indicate swollen polymer conformations comparable to a non-localized polymer and red/orange squares shrunk polymers during localization with a minimum size at $Pe = 100$ (orange).

swelling of the polymer with increasing Péclet number, where the swelling is more pronounced at higher ABP concentrations. At small Pe, the interactions with the ABPs seem to result in a small shrinkage of the polymer, an effect that appears also for polymers composed of ABP monomers (ABPOs) in the presence of excluded-volume interactions [84–86]. Qualitative, the conformational properties are similar to those of ABPOs [74, 77]. However, ABPOs swell stronger and reach asymptotically the value $\langle \boldsymbol{R}_e^2 \rangle / L^2 \approx 0.4$ in the limit $Pe \to \infty$ [76], a value slightly smaller than the theoretically predicted

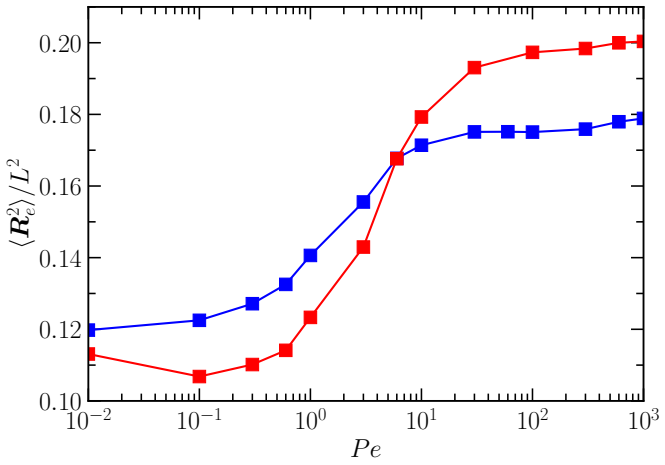

FIG. 4. Mean-square end-to-end distance of a flexible polymer as a function of Péclet number for the ABP packing fractions $\phi = 0.13$ (blue) and $\phi = 0.27$ (red).

value 1/2 [74], whereas here $\langle \boldsymbol{R}_e^2 \rangle / L^2 \approx 0.2$ for $\phi = 0.27$. Hence, qualitatively a passive polymer in an active bath exhibits the same conformational properties as an ABPO, however, to a less extent.

2. *High ABP concentration regime — MIPS*

At high concentrations, we consider $\phi = 0.53$, the ABPs exhibit MIPS associated with strong density differences above a critical Péclet number (Fig. 1 and 3). Most remarkable, the active bath leads to a polymer localization in the bubble of the low-density ABP phase over a certain range of Péclet numbers (red/orange squares in Fig. 3). This is quantified by the fraction of ABPs in a spherical volume centered at the polymer center of mass. Figure 5 presents distribution functions of the packing fraction ϕ_a of ABPs within a sphere of radius $R = 5.5\sigma$ — the radius is much larger than the radius of gyration $R_g \approx 2.7\sigma$ of the flexible polymer in dilute solution — for various Péclet numbers. (The result is independent of R, as an analysis for spheres of radii $R = 5.5 \pm 2$ shows.) At $Pe = 10$, the fluid is homogeneous, the peak in $P(\phi_a)$ corresponds to the average packing fraction. With increasing Pe ($Pe = 40$) the maximum shifts to larger packing fractions and the distribution function broadens [87]. For $Pe = 100$, the distribution function exhibits a peak at $\phi_a \approx 0.23$, with a broad tail toward higher ϕ_a. This reflects a preferred localization of the polymer in the low-density ABP spatial region (Fig. 6). At higher Péclet numbers, phase localization switches and the polymer is dissolved in the high-density ABP phase, as indicated by the peak at $\phi_a \approx 0.6$ for $Pe = 300$ and 600. The inset of Fig. 5 illustrates the substantial drop in the average ABP packing fraction in the vicinity of the polymer at $Pe = 100$. Figure 6 shows various snapshots of polymers in the low- and high-density ABP phase.

The localization of the polymer in the bubble of the dilute ABP region severely affects its conformations. Figure 7 displays the mean square end-to-end distance of semiflexible polymers of various persistence lengths and Péclet numbers. An increasing activity leads to a swelling of flexible ($k_b = 0$) and a shrinkage of semiflexible polymers ($k_b = 2,\ 10$), as for ABPOs [74]. Above $Pe \approx 10$, even passive semiflexible polymers swell with increasing Pe similar to flexible polymers [74]. However, due to localization in the low-density ABP regime, the polymer shrinks for $Pe \gtrsim 40$, assumes a minimum at $Pe \approx 100$, and reswells for larger Péclet numbers. The shrinkage appears as soon as the ABPs phase separate at $Pe \approx 34$ and is most pronounced for $Pe = 100$. Noteworthy, polymers of all considered stiffnesses shrink and reswell in a similar manner. The apparent asymptotic mean square end-to-end distance for $Pe \to \infty$, $\langle \boldsymbol{R}_e^2 \rangle / L^2 \approx 0.3$, is larger than the values in Fig. 4 for the lower ABP concentrations. Hence, the active bath implies qualitatively similar features as those observed for ABPOs, namely swelling of flexible polymers and shrinkage and reswelling of semi-

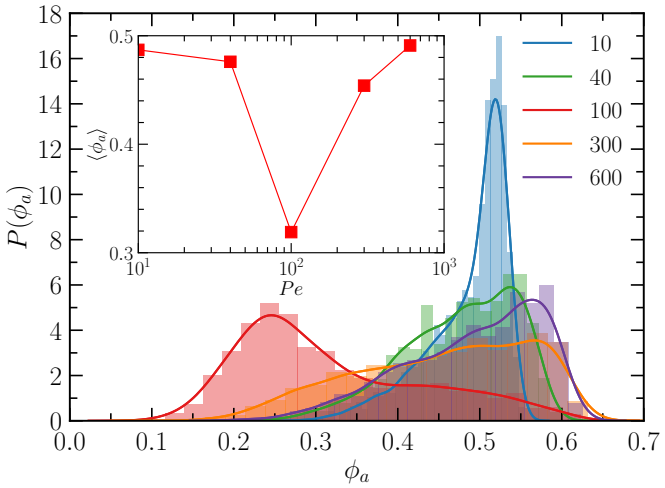

FIG. 5. Distribution function of the local ABP packing fraction within a sphere of radius $R = 5.5\sigma$ centered at the polymer center-of-mass position for the indicated Péclet numbers $Pe = 10 - 600$. Inset: mean value of the local packing fraction as a function of the Péclet number. The average packing fraction is $\phi = 0.53$.

flexible polymers, yet, in addition, it induces a polymer localization over a certain range of Péclet numbers by MIPS.

Two-dimensional mixtures of ABPs and PPs at $Pe = 100$ exhibit an increased concentration of PPs in the ABP depleted phase of the phase-separated mixture [42]. The same physical mechanism may apply for ABP/polymer and ABP/PP mixtures, although the density of the ABP/PP mixture is much higher in the studies of Ref. [42] and the Péclet-number dependence has not be studied, i.e., it is not clear whether a higher density of PPs in the ABP rich phase would be obtained at high Péclet numbers. Interestingly, the polymers approximately assume the same size as a flexible polymers in dilute solution. This is surprising, since polymers in a homogeneous active bath of the density of the dilute regime ($\phi = \phi_a \approx 0.32$, Fig. 5) are substantially swollen as shown in Fig. 4. Thus, segregation is not the only reason for the strong polymer shrinkage. The polymer is highly dynamic and rapidly explores the low-density ABP bubble. Yet, it is most of the time localized inside that bubble. The ABPs in the high density phase seem to repel the polymer, which may ultimately be responsible for its strong shrinkage. Only beyond a certain Péclet number, the active forces are strong enough to overcome the activity-induced confinement.

B. Polymer dynamical properties

1. *Low ABP concentration regime — homogeneous fluid*

Results for the polymer center-of-mass dynamics at ABP packing fractions below the critical value $\phi \approx 0.34$ are displayed in Fig. 8. The active bath implies an enhanced dynamics with a Pe-dependent short-time superdiffusive regime (Fig. 8(a)), yet, with an exponent smaller than 2, and long-time diffusion with an activity-amplified diffusion coefficient. As for the passive particles in the active bath, the crossover to the diffusive regime shifts to shorter times with increasing Pe.

The extracted long-time activity-enhanced diffusion coefficients are depicted in Fig. 8(b). They increase in a power-law manner with increasing Péclet number, with an exponent depending on the ABP concentration. The exponents, 1.30 and 1.38, are larger than those of passive particles in the active bath (Fig. 2), but are smaller than the value 2.0 (black line) of ABPOs in dilute solution [75, 77]. Hence, the active bath yields an enhanced diffusive motion of polymers, qualitatively similar to ABPOs, however with significant quantitative differences in terms of activity-dependence and magnitude, as reflected by the variance with diffusion coefficients of ABPOs (black line in Fig. 8). This can be considered as a consequence of a finite and short lived cooperative motion of an ABP and a monomer. ABPs push against monomers for a short time before the slide past of them, which implies an effectively smaller Péclet number and an effective active noise different from strict colored nose.

Diffusion of a polymer in a passive bath is determined by the bath temperature, and the dissipation-fluctuation relation applies. The existence of a comparable effective temperature and relation is a priori not evident and various contradicting cases have been presented and discussed for active systems [17, 88–91]. The center-of-mass MSD of a passive polymer with inertia in a white-noise bath is given by [92]

$$\left\langle \Delta \boldsymbol{r}_{cm}^2(t) \right\rangle = \frac{6D_e}{\gamma} \left(\gamma t - 1 + e^{-\gamma t} \right), \qquad (11)$$

with the diffusion coefficient $D_e = k_B T_e/(M\gamma)$, the temperature T_e, and the total polymer mass M. Equation (11) shows a universal time-dependent function with the argument γt, multiplied by a temperature-dependent factor. The MSDs of Fig. 8(a) cannot be reproduced by Eq. (11) for an activity-independent friction coefficient, as the short-time power-law changes with activity and the crossover to diffusion shifts to shorter times with increasing Pe. Hence, the overall polymer dynamics cannot be described by an effective temperature in general. However, in the diffusive regime, $t/\tau \gtrsim 10^2$, the active diffusion coefficient can be related to a temperature T_e, and with $D = D_e$ follows $T_e \sim Pe^{\alpha}$, with $\alpha = 1.30$ and 1.38 for the packing fractions $\phi = 0.13$ and 0.27, respectively. The power-law relation is rather trivial and no conclusions on the underlying stochastic process can be drawn, and, hence, on the existence of an effective temperature.

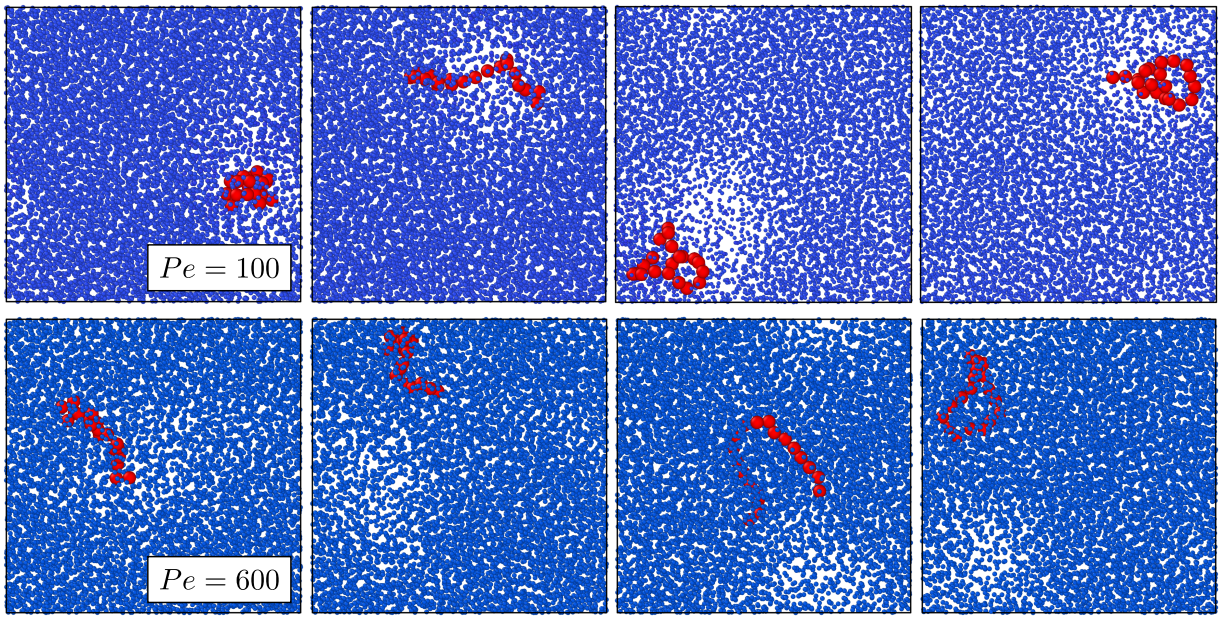

FIG. 6. Snapshots illustrating the localization of the polymer in the dilute (top, $Pe = 100$) and dense (bottom, $Pe = 600$) ABP phase, respectively, at various times. The average packing fraction is $\phi = 0.53$. (See movies M1 and M2 of the supplementary material for illustration.)

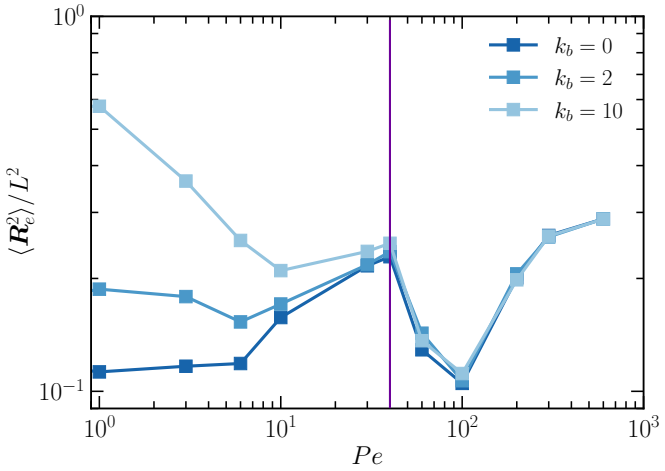

FIG. 7. Mean square end-to-end distance of semiflexible polymers of length $L = 19l$ as a function of Pe. The ABP fluid density is $\phi = 0.53$ and the stiffness parameters of the bending potential are indicated in the legend. The purple line at $Pe = 40$ approximately indicates the critical Péclet number for MPIS (cf. Fig. 3).

2. *High ABP concentration regime — MIPS*

The phase separation of the ABPs and the associated localization of the polymer in the low-density phase affects the polymer dynamics. Figure 9(a) displays polymer center-of-mass mean-square displacements for various Péclet numbers. As for the lower ABP densities, the MSD exhibits an activity-dependent subdiffusive short-time regime with the time dependence $t^{1.6}$ followed by diffusion at longer times. Remarkably, the MSD curve for $Pe = 10^2$ shows a slow-down of the polymer dynamics compared to that for somewhat smaller and larger Pe, which is related to the localization of the polymer in the low-density ABP bubble (Fig. 5). Although the local polymer dynamics is rather fast, the long-time behavior is determined by the diffusive dynamics of the low-density ABP bubble. The center-of-mass diffusion coefficients displayed in Fig. 9(b) emphasize the changes of the polymer dynamics in the vicinity and above the critical Péclet number for MIPS. For $Pe = 40$, close to the MIPS transition, we find an enhanced polymer dynamics compared to the "average" trend revealed by the power-law $Pe^{1.75}$. Here, larger density fluctuations seem to result in an additional active noise leading to a faster dynamics. At $Pe \approx 10^2$, the polymer diffuses, at least part time, with the low-density ABP bubble, which moves significantly slower due to collective effects. The dissolution of the polymer for activities $Pe \gtrsim 2 \times 10^2$ in the high ABP-density region results in an enhanced diffusion. The activity dependence, $Pe^{1.75}$, is similar for $Pe < 30$ and $Pe \gtrsim 10^2$, since the average ABP concentrations in the vicinity of the polymer are comparable as reflected in Fig. 5.

We like to emphasize that MSD curves and diffusion coefficients of semiflexible polymers (Fig. 7) are indistinguishable from those of the flexible polymer (Fig. 9) for the presented range of activities. The strong conformational change by the active bath render stiffness irrelevant.

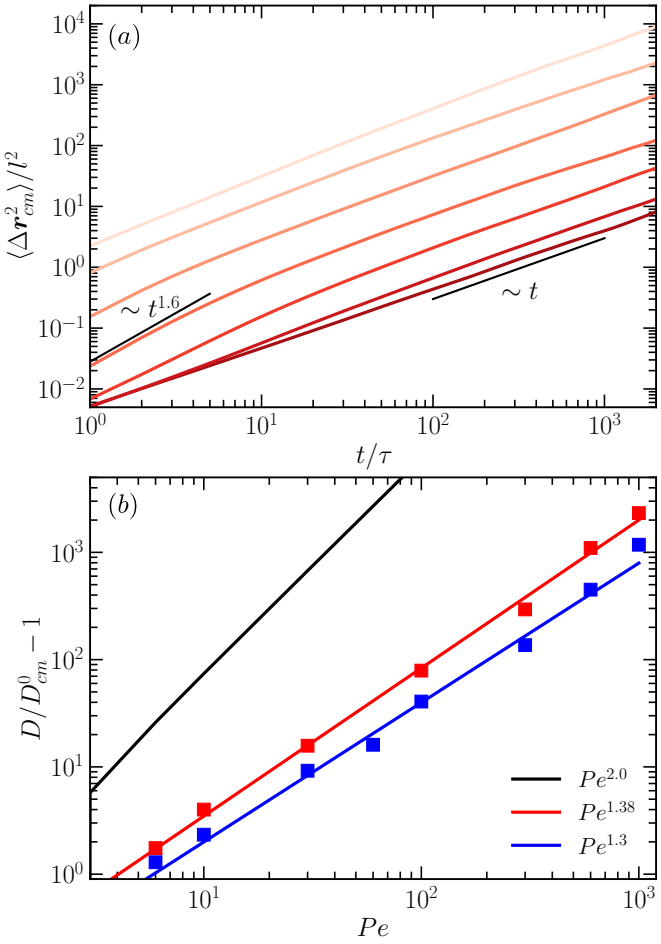

FIG. 8. (a) Center-of-mass mean-square displacement as a function of time of a flexible polymer in an ABP bath of packing fraction $\phi = 0.27$ for the Péclet numbers $Pe = 1$, 3, 10, 30, 100, 300, and 600 (dark to light). The black lines indicate (fitted) power-law dependencies. (b) Diffusion coefficients extracted from the long-time diffusive regime for the ABP packing fractions $\phi = 0.13$ (blue) and 0.27 (red). Symbols indicate simulation results and the corresponding solid lines are power-law fits with the exponents displayed in the legend. The black line denotes the active diffusion coefficient of an ABPO in dilute solution for the same D_R. D_{cm}^0 is the diffusion coefficient of the polymer in a passive bath with $\phi = 0.2$.

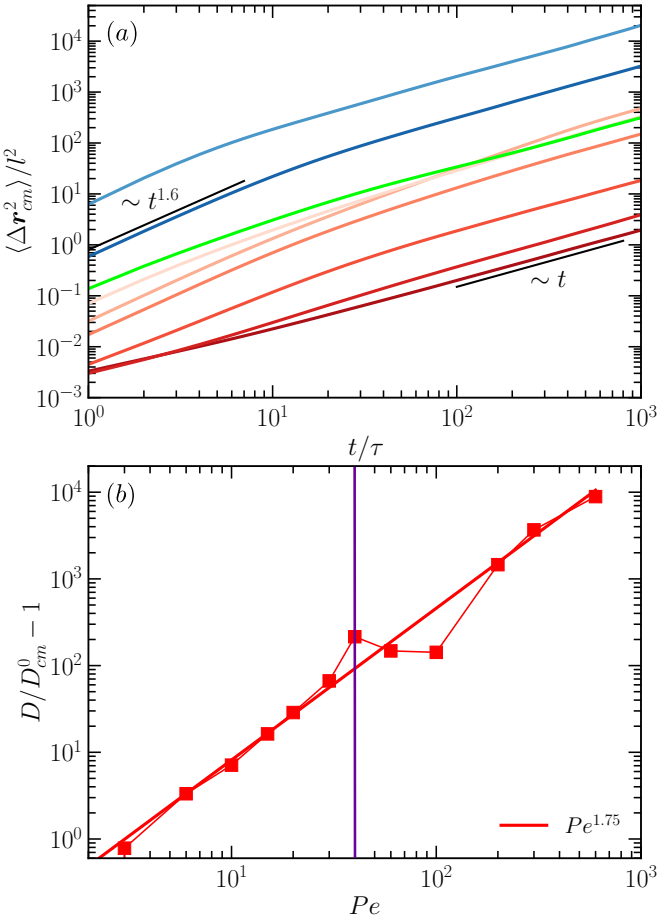

FIG. 9. (a) Center-of-mass mean-square displacement as a function of time of a flexible polymer in an ABP bath of packing fraction $\phi = 0.53$ for the Péclet numbers $Pe = 1$, 3, 10, 30, 40, 60 (red, dark to light), 100 (lime), 300, and 600 (blue, dark to light). The black lines indicate (fitted) power-law dependencies. (b) Diffusion coefficients extracted from the long-time diffusive regime. Symbols indicate simulation results with the thin solid line as a guide for the eye. The thick solid line indicates the fitted power-law increase $Pe^{1.75}$. The purple line at $Pe = 40$ approximately indicates the critical Péclet number for MIPS (cf. Fig. 3).

V. SUMMARY AND CONCLUSIONS

We have performed computer simulations of mixtures of isometric passive colloids and active Brownian particles (ABPs) as well as of a passive polymer embedded in an ABP bath for various ABP packing fractions, ϕ, and activities, Pe. In general, the active bath strongly affects the embedded passive particles, with a pronounced enhancement of their dynamics.

Our simulations of mixtures of isometric passive and active particles at the total packing fraction $\phi = 0.53$ and the fraction of passive particles in the range $N_p/N = 0.3 - 0.5$ show no large-scale phase separation. For the latter, higher APB concentrations are required. The ABP bath enhances the dynamics of the passive particles, with a 30% faster diffusion for $N_p/N = 0.3$ compared to the ratio $N_p/N = 0.5$. For any considered ratio N_p/N, the diffusion coefficient of the passive particles increases as $P^{1.16}$ with increasing Péclet number in the range $3 \leq Pe \leq 300$. However, the ABP dynamics is independent of the concentration of the passive particles in the considered range and their active diffusion coefficient increases as $Pe^{1.6}$ with increasing Pe.

Our studies of a single polymer in an ABP bath of packing fraction $\phi = 0.13$ and 0.27 — both densities are below the critical value for MIPS — and $Pe \lesssim 300$ reveal swelling of the polymer with increasing Péclet num-

ber, which saturates for $Pe \gtrsim 20$. Here, swelling is more pronounced for higher ABP concentrations. As for passive monomers, the dynamics is enhanced and the diffusion coefficient increase in a power-law manner for $1 < Pe \lesssim 10^3$ with an ABP density-dependent exponent.

Remarkably, for the ABP packing fraction $\phi = 0.53$, we find localization of the polymer in the low-density spatial region — in fact, a low density bubble — of the phase separated ABP bath at $Pe \approx 10^2$. This separation is accompanied by a collapse of the originally activity-swollen polymer to a value comparable to that of the flexible polymer in the passive bath. Noteworthy, this collapse is independent of polymer stiffness, at least over a significant range of stiffnesses. For larger $Pe \gtrsim 2 \times 10^2$, the polymer is no longer localized and therefore swells again, approaching asymptotically a constant value for large Pe. The localization process also affects the polymer dynamics, and the diffusion coefficient in the localized state is significantly smaller than that predicted in absence of phase separation.

Quantitatively, the properties of a polymer in an active bath are significantly different from those of a polymer comprised of ABP monomers (ABPO) [74, 75, 77]. Common to both is the change of the conformations by swelling and an enhanced dynamics. However, there are major quantitative differences in terms of strength of the obtained effects and the dependence on the (effective) Péclet number. Here, the passive polymers shows significantly smaller effects and, in power-laws, smaller exponents. This is a consequence of the far less persistent motion of passive particles in an active bath compered to, e.g., ABP monomers of an ABPO. Ultimately, the active bath does not correspond to a colored-noise external source in this case [75] due to the only short-time correlated motion of ABPs and monomers, shorter than the characteristic time of the colored noise of the ABPs,

Yet, the bath does not correspond to a thermal bath either, and, strictly speaking, no effective temperature can be introduced. The comparison of the polymer center-of-mass mean-square displacements at $\phi = 0.27$ (Fig. 8) with its theoretical prediction in a thermal bath clearly reveals a more complex dynamics in the active bath. A similar qualitative behavior is displayed by passive particles in an active bath. An effective temperature, T_e, can be introduced to account for the activity dependence of the diffusion coefficient, though with a nonlinear relation between T_e and Pe. Specifically the concentration-dependent exponent of the latter relation indicates a more complex fluctuation-dissipation-like relation of the active bath than a thermal (white-noise) bath.

Our simulation study is a first step toward the elucidation of the complex interplay between an active bath and embedded polymers or filaments. We hope that they stimulate further investigations, specifically taking into account several polymers, which might show aggregation in the low-density regions of the APB bath.

SUPPLEMENTARY MATERIAL

The supplementary material provides movies of the polymer dynamics in the active bath. Movie M1 illustrates the dynamics for $Pe = 100$ and M2 for $Pe = 600$.

DATA AVAILABILITY

The data that support the findings of this study are available from the corresponding authors upon reasonable request.

[1] H. P. Zhang, A. Be'er, R. S. Smith, E. L. Florin, and H. L. Swinney, Swarming dynamics in bacterial colonies, *EPL (Europhysics Letters)*, Europhys. Lett. **87**, 48011 (2009).

[2] N. C. Darnton, L. Turner, S. Rojevsky, and H. C. Berg, Dynamics of bacterial swarming, Biophys. J. **98**, 2082 (2010).

[3] C. Dombrowski, L. Cisneros, S. Chatkaew, R. E. Goldstein, and J. O. Kessler, Self-concentration and large-scale coherence in bacterial dynamics, Phys. Rev. Lett. **93**, 098103 (2004).

[4] C. W. Wolgemuth, Collective swimming and the dynamics of bacterial turbulence, Biophys. J. **95**, 1564 (2008).

[5] J. Gachelin, A. Rousselet, A. Lindner, and E. Clement, Collective motion in an active suspension ofescherichia colibacteria, New J. Phys. **16**, 025003 (2014).

[6] J. Dunkel, S. Heidenreich, K. Drescher, H. H. Wensink, M. Bär, and R. E. Goldstein, Fluid dynamics of bacterial turbulence, Phys. Rev. Lett. **110**, 228102 (2013).

[7] K. Beppu, Z. Izri, J. Gohya, K. Eto, M. Ichikawa, and Y. T. Maeda, Geometry-driven collective ordering of bacterial vortices, Soft Matter **13**, 5038 (2017).

[8] A. Sokolov and I. S. Aranson, Physical properties of collective motion in suspensions of bacteria, Phys. Rev. Lett. **109**, 248109 (2012).

[9] H. H. Wensink, J. Dunkel, S. Heidenreich, K. Drescher, R. E. Goldstein, H. Löwen, and J. M. Yeomans, Mesoscale turbulence in living fluids, Proc. Natl. Acad. Sci. USA **109**, 14308 (2012).

[10] R. Colin, K. Drescher, and V. Sourjik, Chemotactic behaviour of escherichia coli at high cell density, Nat. Commun. **10**, 5329 (2019).

[11] A. Be'er, B. Ilkanaiv, R. Gross, D. B. Kearns, S. Heidenreich, M. Bär, and G. Ariel, A phase diagram for bacterial swarming, Commun. Phys. **3**, 66 (2020).

[12] K. Qi, G. Gompper, and R. G. Winkler, submitted for publication (2021).

[13] G. Gompper, R. G. Winkler, T. Speck, A. Solon, C. Nardini, F. Peruani, H. Löwen, R. Golestanian, U. B. Kaupp, L. Alvarez, T. Kiørboe, E. Lauga, W. C. K. Poon, A. DeSimone, S. Muiños-Landin, A. Fischer, N. A. Söker, F. Cichos, R. Kapral, P. Gaspard, M. Ripoll, F. Sagues,

A. Doostmohammadi, J. M. Yeomans, I. S. Aranson, C. Bechinger, H. Stark, C. K. Hemelrijk, F. J. Nedelec, T. Sarkar, T. Aryaksama, M. Lacroix, G. Duclos, V. Yashunsky, P. Silberzan, M. Arroyo, and S. Kale, The 2020 motile active matter roadmap, J. Phys: Condens. Matter **32**, 193001 (2020).

[14] M. E. Cates and J. Tailleur, Motility-induced phase separation, Annu. Rev. Condens. Matter Phys. **6**, 219 (2015).

[15] J. Elgeti, R. G. Winkler, and G. Gompper, Physics of microswimmers—single particle motion and collective behavior: a review, Rep. Prog. Phys. **78**, 056601 (2015).

[16] C. Bechinger, R. Di Leonardo, H. Löwen, C. Reichhardt, G. Volpe, and G. Volpe, Active particles in complex and crowded environments, Rev. Mod. Phys. **88**, 045006 (2016).

[17] J. Bialké, T. Speck, and H. Löwen, Crystallization in a dense suspension of self-propelled particles, Phys. Rev. Lett. **108**, 168301 (2012).

[18] G. S. Redner, M. F. Hagan, and A. Baskaran, Structure and dynamics of a phase-separating active colloidal fluid, Phys. Rev. Lett. **110**, 055701 (2013).

[19] Y. Fily, A. Baskaran, and M. F. Hagan, Dynamics of self-propelled particles under strong confinement, Soft Matter **10**, 5609 (2014).

[20] A. Wysocki, R. G. Winkler, and G. Gompper, Cooperative motion of active Brownian spheres in three-dimensional dense suspensions, EPL **105**, 48004 (2014).

[21] J. Stenhammar, D. Marenduzzo, R. J. Allen, and M. E. Cates, Phase behaviour of active Brownian particles: the role of dimensionality, Soft Matter **10**, 1489 (2014).

[22] P. Digregorio, D. Levis, A. Suma, L. F. Cugliandolo, G. Gonnella, and I. Pagonabarraga, Full phase diagram of active Brownian disks: From melting to motility-induced phase separation, Phys. Rev. Lett. **121**, 098003 (2018).

[23] M. R. Shaebani, A. Wysocki, R. G. Winkler, G. Gompper, and H. Rieger, Computational models for active matter, Nat. Rev. Phys. **2**, 181 (2020).

[24] J. T. Siebert, J. Letz, T. Speck, and P. Virnau, Phase behavior of active Brownian disks, spheres, and dimers, Soft Matter **13**, 1020 (2017).

[25] F. Turci and N. B. Wilding, Phase separation and multibody effects in three-dimensional active Brownian particles, Phys. Rev. Lett. **126**, 038002 (2021).

[26] X.-L. Wu and A. Libchaber, Particle diffusion in a quasi-two-dimensional bacterial bath, Phys. Rev. Lett. **84**, 3017 (2000).

[27] M. J. Kim and K. S. Breuer, Enhanced diffusion due to motile bacteria, Phys. Fluids **16**, L78 (2004).

[28] D. T. N. Chen, A. W. C. Lau, L. A. Hough, M. F. Islam, M. Goulian, T. C. Lubensky, and A. G. Yodh, Fluctuations and rheology in active bacterial suspensions, Phys. Rev. Lett. **99**, 148302 (2007).

[29] P. T. Underhill, J. P. Hernandez-Ortiz, and M. D. Graham, Diffusion and spatial correlations in suspensions of swimming particles, Phys. Rev. Lett. **100**, 248101 (2008).

[30] K. C. Leptos, J. S. Guasto, J. P. Gollub, A. I. Pesci, and R. E. Goldstein, Dynamics of enhanced tracer diffusion in suspensions of swimming eukaryotic microorganisms, Phys. Rev. Lett. **103**, 198103 (2009).

[31] T. Ishikawa, J. T. Locsei, and T. J. Pedley, Fluid particle diffusion in a semidilute suspension of model microorganisms, Phys. Rev. E **82**, 021408 (2010).

[32] L. G. Wilson, V. A. Martinez, J. Schwarz-Linek, J. Tailleur, G. Bryant, P. N. Pusey, and W. C. K. Poon, Differential dynamic microscopy of bacterial motility, Phys. Rev. Lett. **106**, 018101 (2011).

[33] H. Kurtuldu, J. S. Guasto, K. A. Johnson, and J. P. Gollub, Enhancement of biomixing by swimming algal cells in two-dimensional films, Proc. Natl. Acad. Sci. USA **108**, 10391 (2011).

[34] G. L. Miño, J. Dunstan, A. Rousselet, E. Clément, and R. Soto, Induced diffusion of tracers in a bacterial suspension: theory and experiments, J. Fluid Mech. **729**, 423 (2013).

[35] A. Morozov and D. Marenduzzo, Enhanced diffusion of tracer particles in dilute bacterial suspensions, Soft Matter **10**, 2748 (2014).

[36] T. V. Kasyap, D. L. Koch, and M. Wu, Hydrodynamic tracer diffusion in suspensions of swimming bacteria, Phys. Fluids **26**, 081901 (2014).

[37] Y. Peng, L. Lai, Y.-S. Tai, K. Zhang, X. Xu, and X. Cheng, Diffusion of ellipsoids in bacterial suspensions, Phys. Rev. Lett. **116**, 068303 (2016).

[38] B. Delmotte, E. E. Keaveny, E. Climent, and F. Plouraboué, Simulations of Brownian tracer transport in squirmer suspensions, IMA J. Appl. Math. **83**, 680 (2018).

[39] M. Shafiei Aporvari, M. Utkur, E. U. Saritas, G. Volpe, and J. Stenhammar, Anisotropic dynamics of a self-assembled colloidal chain in an active bath, Soft Matter 10.1039/D0SM00318B (2020).

[40] F. Kümmel, P. Shabestari, C. Lozano, G. Volpe, and C. Bechinger, Formation, compression and surface melting of colloidal clusters by active particles, Soft Matter **11**, 6187 (2015).

[41] J. Stenhammar, R. Wittkowski, D. Marenduzzo, and M. E. Cates, Activity-induced phase separation and self-assembly in mixtures of active and passive particles, Phys. Rev. Lett. **114**, 018301 (2015).

[42] A. Wysocki, R. G. Winkler, and G. Gompper, Propagating interfaces in mixtures of active and passive Brownian particles, New J. Phys. **18**, 123030 (2016).

[43] D. R. Rodriguez, F. Alarcón, R. Martinez, J. Ramírez, and C. Valeriani, Phase behaviour and dynamical features of a two-dimensional binary mixture of active/passive spherical particles, Soft Matter **16**, 1162 (2020).

[44] B. van der Meer, V. Prymidis, M. Dijkstra, and L. Filion, Predicting the phase behavior of mixtures of active spherical particles, J. Chem. Phys. **152**, 144901 (2020).

[45] P. Dolai, A. Simha, and S. Mishra, Phase separation in binary mixtures of active and passive particles, Soft Matter **14**, 6137 (2018).

[46] A. Y. Grosberg and J. F. Joanny, Nonequilibrium statistical mechanics of mixtures of particles in contact with different thermostats, Phys. Rev. E **92**, 032118 (2015).

[47] S. N. Weber, C. A. Weber, and E. Frey, Binary mixtures of particles with different diffusivities demix, Phys. Rev. Lett. **116**, 058301 (2016).

[48] D. Bray, *Cell movements: from molecules to motility* (Garland Science, 2000).

[49] K. Roberts, B. Alberts, A. Johnson, P. Walter, and T. Hunt, *Molecular biology of the cell* (Garland Science, 2002).

[50] D. A. Fletcher and P. L. Geissler, Active biological materials, Annu. Rev. Phys. Chem. **60**, 469 (2009).

[51] D. Saintillan, M. J. Shelley, and A. Zidovska, Extensile motor activity drives coherent motions in a model of in-

terphase chromatin, Proc. Natl. Acad. Sci. USA **115**, 11442 (2018).
[52] J. I. Prosser, B. J. M. Bohannan, T. P. Curtis, R. J. Ellis, M. K. Firestone, R. P. Freckleton, J. L. Green, L. E. Green, K. Killham, J. J. Lennon, A. M. Osborn, M. Solan, C. J. van der Gast, and J. P. W. Young, The role of ecological theory in microbial ecology, Nat. Rev. Microbiol. **5**, 384 (2007).
[53] E. Kunze, J. F. Dower, I. Beveridge, R. Dewey, and K. P. Bartlett, Observations of biologically generated turbulence in a coastal inlet, Science **313**, 1768 (2006).
[54] S. Roman and S. J. R., Ecology and physics of bacterial chemotaxis in the ocean, Microbiol. Mol. Biol. Rev. **76**, 792 (2012).
[55] A. Caspi, R. Granek, and M. Elbaum, Enhanced diffusion in active intracellular transport, Phys. Rev. Lett. **85**, 5655 (2000).
[56] C. P. Brangwynne, G. H. Koenderink, F. C. MacKintosh, and D. A. Weitz, Cytoplasmic diffusion: molecular motors mix it up, J. Cell. Biol. **183**, 583 (2008).
[57] M. Guo, A. J. Ehrlicher, M. H. Jensen, M. Renz, J. R. Moore, R. D. Goldman, J. Lippincott-Schwartz, F. C. Mackintosh, and D. A. Weitz, Probing the stochastic, motor-driven properties of the cytoplasm using force spectrum microscopy, Cell **158**, 822 (2014).
[58] A. S. Mikhailov and R. Kapral, Hydrodynamic collective effects of active protein machines in solution and lipid bilayers, Proc. Natl. Acad. Sci. USA **112**, E3639 (2015).
[59] S. C. Weber, A. J. Spakowitz, and J. A. Theriot, Nonthermal ATP-dependent fluctuations contribute to the in vivo motion of chromosomal loci, Proc. Natl. Acad. Sci. USA **109**, 7338 (2012).
[60] W. Lu, M. Winding, M. Lakonishok, J. Wildonger, and V. I. Gelfand, Microtubule–microtubule sliding by kinesin-1 is essential for normal cytoplasmic streaming in *Drosophila* oocytes, Proc. Natl. Acad. Sci. USA **113**, E4995 (2016).
[61] J. Smrek and K. Kremer, Small activity differences drive phase separation in active-passive polymer mixtures, Phys. Rev. Lett. **118**, 098002 (2017).
[62] E. Lieberman-Aiden, N. L. van Berkum, L. Williams, M. Imakaev, T. Ragoczy, A. Telling, I. Amit, B. R. Lajoie, P. J. Sabo, M. O. Dorschner, R. Sandstrom, B. Bernstein, M. A. Bender, M. Groudine, A. Gnirke, J. Stamatoyannopoulos, L. A. Mirny, E. S. Lander, and J. Dekker, Comprehensive mapping of long-range interactions reveals folding principles of the human genome, Science **326**, 289 (2009).
[63] T. Cremer, M. Cremer, B. Hübner, H. Strickfaden, D. Smeets, J. Popken, M. Sterr, Y. Markaki, K. Rippe, and C. Cremer, The 4d nucleome: Evidence for a dynamic nuclear landscape based on co-aligned active and inactive nuclear compartments, FEBS Lett. **589**, 2931 (2015).
[64] I. Solovei, K. Thanisch, and Y. Feodorova, How to rule the nucleus: divide et impera, *Cell nucleus*, Current Opinion in Cell Biology **40**, 47 (2016).
[65] N. Ganai, S. Sengupta, and G. I. Menon, Chromosome positioning from activity-based segregation, Nucleic Acids Res. **42**, 4145 (2014).
[66] C. P. Brangwynne, T. J. Mitchison, and A. A. Hyman, Active liquid-like behavior of nucleoli determines their size and shape in *xenopus laevis* oocytes, Proc. Natl. Acad. Sci. USA **108**, 4334 (2011).
[67] H. Falahati and E. Wieschaus, Independent active and thermodynamic processes govern the nucleolus assembly in vivo, Proc. Natl. Acad. Sci. USA **114**, 1335 (2017).
[68] W. M. Babinchak and W. K. Surewicz, Liquid–liquid phase separation and its mechanistic role in pathological protein aggregation, J. Mol. Biol. 10.1016/j.jmb.2020.03.004 (2020).
[69] J. Harder, C. Valeriani, and A. Cacciuto, Activity-induced collapse and reexpansion of rigid polymers, Phys. Rev. E **90**, 062312 (2014).
[70] A. Kaiser and H. Löwen, Unusual swelling of a polymer in a bacterial bath, J. Chem. Phys. **141**, 044903 (2014).
[71] N. Nikola, A. P. Solon, Y. Kafri, M. Kardar, J. Tailleur, and R. Voituriez, Active particles with soft and curved walls: Equation of state, ratchets, and instabilities, Phys. Rev. Lett. **117**, 098001 (2016).
[72] Y.-q. Xia, Z.-l. Shen, W.-d. Tian, and K. Chen, Unfolding of a diblock chain and its anomalous diffusion induced by active particles, J. Chem. Phys. **150**, 154903 (2019).
[73] Y.-Q. Xia, W.-D. Tian, K. Chen, and Y.-Q. Ma, Globule–stretch transition of a self-attracting chain in the repulsive active particle bath, Phys. Chem. Chem. Phys. **21**, 4487 (2019).
[74] T. Eisenstecken, G. Gompper, and R. G. Winkler, Conformational properties of active semiflexible polymers, Polymers **8**, 304 (2016).
[75] T. Eisenstecken, G. Gompper, and R. G. Winkler, Internal dynamics of semiflexible polymers with active noise, J. Chem. Phys. **146**, 154903 (2017).
[76] A. Martin-Gomez, T. Eisenstecken, G. Gompper, and R. G. Winkler, Hydrodynamics of polymers in an active bath, Phys. Rev. E **101**, 052612 (2020).
[77] R. G. Winkler and G. Gompper, The physics of active polymers and filaments, *The Journal of Chemical Physics*, J. Chem. Phys. **153**, 040901 (2020).
[78] P. Hänggi and P. Jung, Colored noise in dynamical systems, Adv. Chem. Phys. **89**, 239 (1995).
[79] A. P. Solon, J. Stenhammar, R. Wittkowski, M. Kardar, Y. Kafri, M. E. Cates, and J. Tailleur, Pressure and phase equilibria in interacting active Brownian spheres, Phys. Rev. Lett. **114**, 198301 (2015).
[80] S. Das, G. Gompper, and R. G. Winkler, Confined active Brownian particles: theoretical description of propulsion-induced accumulation, New J. Phys. **20**, 015001 (2018).
[81] R. G. Winkler, A. Wysocki, and G. Gompper, Virial pressure in systems of spherical active Brownian particles, Soft Matter **11**, 6680 (2015).
[82] N. Grønbech-Jensen and O. Farago, A simple and effective Verlet-type algorithm for simulating Langevin dynamics, Mol. Phys. **111**, 983 (2013).
[83] A. Martín-Gómez, T. Eisenstecken, G. Gompper, and R. G. Winkler, Active Brownian filaments with hydrodynamic interactions: conformations and dynamics, Soft Matter **15**, 3957 (2019).
[84] S. K. Anand and S. P. Singh, Conformation and dynamics of a self-avoiding active flexible polymer, Phys. Rev. E **101**, 030501 (2020).
[85] S. Das, N. Kennedy, and A. Cacciuto, The coil–globule transition in self-avoiding active polymers, Soft Matter **17**, 160 (2021).
[86] T. Eisenstecken, A. Ghavami, A. Mair, G. Gompper, and R. G. Winkler, Conformational and dynamical properties of semiflexible polymers in the presence of active noise, AIP Conf. Proc. **1871**, 050001 (2017).

[87] M. Theers, E. Westphal, K. Qi, R. G. Winkler, and G. Gompper, Clustering of microswimmers: interplay of shape and hydrodynamics, Soft Matter **14**, 8590 (2018).
[88] J. Palacci, C. Cottin-Bizonne, C. Ybert, and L. Bocquet, Sedimentation and effective temperature of active colloidal suspensions, Phys. Rev. Lett. **105**, 088304 (2010).
[89] D. Loi, S. Mossa, and L. F. Cugliandolo, Non-conservative forces and effective temperatures in active polymers, Soft Matter **7**, 10193 (2011).
[90] S. Wang and P. G. Wolynes, Communication: Effective temperature and glassy dynamics of active matter, J. Chem. Phys. **135**, 051101 (2011).
[91] Y. Fily and M. C. Marchetti, Athermal phase separation of self-propelled particles with no alignment, Phys. Rev. Lett. **108**, 235702 (2012).
[92] H. Risken, *The Fokker-Planck Equation* (Springer, Berlin, 1989).